Systematic investigation of nucleon optical model potentials in (p, d) transfer reactions*

Silu Chen (陈思璐)[1] Zixuan Liu (刘子旋)[1] Zhi Zhang (张智)[2] Ruirui Xu (续瑞瑞)[2]
Danyang Pang (庞丹阳)[3] Yiping Xu (许祎萍)[1†]

[1]School of Nuclear Science and Engineering, North China Electric Power University, Beijing 102206, China
[2]China Nuclear Data Center, China Institute of Atomic Energy, Beijing 102413, China
[3]School of Physics, Beihang University, Beijing 100191, China

Abstract: The consistent three-body model reaction methodology (TBMRM) proposed by J. Lee *et al.* [Phys. Rev. C 69, 064313 (2004); Phys. Rev. C 73, 044608 (2006); Phys. Rev. C 75, 064320 (2007)], which includes adopting the simple zero-range adiabatic wave approximation, constraining the single-particle potentials using modern Hartree–Fock calculations, and using global nucleon optical model potential (OMP) geometries, are widely applied in systematic studies of transfer reactions. In this study, we investigate the influence of different nucleon OMPs in extracting spectroscopic factors (SFs) from (p,d) reactions. Our study covers 32 sets of angular distribution data of (p,d) reactions on four targets and a large range of incident energies (20-200 MeV/nucleon). This study uses two semi-microscopic nucleon OMPs, i.e., Jeukenne, Lejeune, and Mahaux (JLM) [Phys. Rev. C 16, 80 (1977); Phys. Rev. C 58, 1118 (1998)] and CTOM [Phys. Rev. C 94, 034606 (2016)], and a pure microscopic nucleon potential, i.e., WLH [Phys. Rev. Lett. 127, 182502 (2021)]. The results are compared with those using the phenomenological global optical potential KD02 [Nucl. Phys. A 713, 231 (2003)]. We find that the incident energy dependence of spectroscopic factors extracted from (p,d) reactions is evidently suppressed when microscopic OMPs are employed for ^{12}C, ^{28}Si, and ^{40}Ca. In addition, spectroscopic factors extracted using the systematic microscopic optical potential CTOM based on the Dirac-Brueckner-Hartree-Fock theory are more in line with the results obtained from (e,$e'p$) measurements, except for ^{16}O and ^{40}Ca at high energies (> 100 MeV), necessitating an exact treatment of double-magic nuclei. The results obtained by using the pure microscopic optical potential, WLH, based on the EFT theory show the same trend as those of CTOM but are generally higher. The JLM potential, which relies on simplified nuclear matter calculations with old-fashioned bare interactions, produces results that are very similar to those of the phenomenological potential KD02. Our results indicate that modern microscopic OMPs are reliable tools for probing the nuclear structure using transfer reactions across a wide energy range.

Keywords: optical model potentials, transfer reactions, spectroscopic factors

DOI: 10.1088/1674-1137/ad4269

I. INTRODUCTION

Spectroscopic factors (SFs), which describe the strengths of single-particle states at the Fermi surface of shell closures or quasi-particles, are traditionally considered a link between nuclear reaction and structure studies [1]. For example, SF quenching is an important subject (see review [2] and the references therein) because it is generally suggested to originate from nucleon-nucleon (NN) correlations. Single nucleon transfer reactions, such as (p,d) and (d,p) reactions, have been the primary SF extraction tools over the decades. However, an important issue remains: the SFs extracted from transfer reactions show large uncertainties resulting from experimental measurements [3] and theoretical predictions [4–8]. The latter uncertainty type is typically associated with the choice of reaction models, optical model potentials (OMPs), and single-particle potential (SPP) parameters. Thus, the increasing interest in using single-nucleon transfer reactions to probe nuclear structures and astrophysical information has fostered an ongoing need to evaluate the accuracy of conventional methods for transfer reactions throughout a wide energy range.

J. Lee and J. A. Tostevin *et al.* developed a consistent

Received 16 September 2023; Accepted 23 April 2024; Published online 24 April 2024

* Supported by the National Natural Science Foundation of China (U2067205, 12205098), and the National Key Research and Development Program of China (2022YFA1602403)

† E-mail: xuyp_snse@ncepu.edu.cn

three-body model reaction methodology (TBMRM) to analyze (p,d) and (d,p) reactions [9–13] to address this problem, and their approach has effectively improved the consistency of SFs extracted from transfer reactions. The methodology includes adopting the zero-range adiabatic wave approximation (ZR-ADWA) [14], constraining the SPP parameters by modern Hartree–Fock (HF) calculations, and using global nucleon optical potentials that can be applied consistently at all the required incident energies and for all targets, for example, OMPs derived by folding the effective nucleon-nucleon interaction of Jeukenne, Lejeune, and Mahaux (JLM) [15, 16] with the nucleon density distributions from the same HF calculations. However, this methodology has some limitations when applying it widely to (p,d) and (d,p) reactions.

Firstly, most systematic TBMRM analyses are performed at relatively low energies (about 5−30 MeV/nucleon). However, unexpected energy dependencies were noted for the SFs extracted from higher energy experimental data [17, 18]. Considering the energy-dependence of OMPS and the validity of adiabatic approximation [19, 20], studying the effects on the nuclear structure information extracted from experimental data within a wide energy range is crucial. In addition, according to our previous work, nucleon elastic scattering and transfer reactions are sensitive to different OMP regions [21]. Therefore, global nucleon OMPs, primarily constrained by elastic scattering cross sections, may not be sufficient for transfer reactions.

In our previous work [21], we suggested using microscopic OMPs reflecting more theoretical considerations rather than phenomenological ones in direct nuclear reaction calculations. Moreover, the available experimental data and microscopic OMPs available have recently become more significant. For instance, a systematic microscopic optical potential CTOM was proposed by R. R. Xu *et al.* [22], based on the Dirac-Brueckner-Hartree-Fock theory. Lately, T. R. Whitehead, Y. Lim, and J. W. Holt constructed a microscopic global nucleon-nucleus optical potential based on an analysis of 1800 isotopes in the many-body perturbation theory framework with state-of-the-art nuclear interactions from chiral effective field theory (EFT) [23]. An attractive feature of the WLH potential is that none of its parameters are fitted to nucleon-nucleus scattering data. One might expect that, being fully derived microscopically, the new microscopic potential might be more suited to probing nuclear structure information via transfer reactions, although OMPs with different parameter sets can usually reproduce the scattering cross section equally well. Therefore, testing the CTOM and WLH potential with (p,d) transfer reactions to see how their results compare with the same calculations using phenomenological global nucleon-nucleus potentials is necessary. In addition, studies on transfer reactions beyond 70 MeV/nucleon are limited, although most global systematic OMPs for nucleons are valid up to 200 MeV/nucleon. Therefore, we analyze the available experimental data, including 32 sets of the angular distributions of (p,d) reactions on ^{12}C, ^{16}O, ^{28}Si and ^{40}Ca for an incident energy range of up to 200 MeV/nucleon. Different OMPs (three microscopic sets and one phenomenological set) are applied in this study within the ADWA framework. This study aims to investigate the effects of different OMPs on the nuclear structure information extracted from (p,d) experimental data over a wide energy range.

II. MODEL CALCULATIONS

Most commonly used global systematic nucleon OMPs are currently limited to 200 MeV/nucleon. Thus, experimental (p,d) differential cross section data available below 200 MeV/nucleon are used to investigate the systematic behavior of SFs in the widest possible incident energy range for the $^{12}C_{g.s.}(p,d)^{11}C_{g.s.}$, $^{16}O_{g.s.}(p,d)^{15}O_{g.s.}$, $^{28}Si_{g.s.}(p,d)^{27}Si_{g.s.}$, and $^{40}Ca_{g.s.}(p,d)^{39}Ca_{g.s.}$ reactions. The choice of the target nuclei is mainly limited by the applicability of the method. As the HF is less appropriate for describing the single-particle configurations of very light systems, we limit the target masses to $A > 11$. Additionally, the reaction mechanism of light nuclei is relatively simple; in the light nuclei, the spin-orbit interaction effect in constructing the valence neutron wave function is of the order of 10% or less [24]. Finally, considering the experimental data availability, we select four targets. The experimental data analyzed in this study are listed in Table 2. All the experimental data were taken from the nuclear reaction database EXFOR/CSISRS [25] or digitized from their original references [26–31].

We adopted and developed the three-body model reaction methodology (TBMRM) proposed by J. Lee *et al.* to analyze (p,d) reactions [10, 11, 13]. This methodology employs the Johnson-Soper ADWA model [14] for the (p,d) and (d,p) reactions, for which the amplitude of a $A(p,d)B$ reaction reads [5]

$$T_{pd} = S F_{nlj}^{1/2} \langle \chi_{dB}^{(-)} \phi_{np} | V_{np} | \chi_{pA}^{(+)} \phi_{nlj} \rangle, \tag{1}$$

where SF_{nlj} is the spectroscopic factor, with n, l, and j being the principal quantum number, angular momentum, and total angular momentum, respectively, of the single neutron wave function ϕ_{nlj} in the nucleus A $(A = B + n)$. χ_{pA} and χ_{dB} are entrance- and exit-channel distorted waves, and V_{np} is the neutron-proton interaction supporting the bound state of the n-p pair ϕ_{np} (the deuteron wave function).

The exit-channel distorted waves are generated using the finite-range (FR) ADWA model, with the following effective "deuteron" (as a subsystem comprising a neut-

ron and proton) potential [14, 32]:

$$U_{dB}(R) = \frac{\langle\phi_{np}|V_{np}\left[U_{nB}(\vec{R}+\frac{\vec{r}}{2})+U_{pB}(\vec{R}-\frac{\vec{r}}{2})\right]|\phi_{np}\rangle}{\langle\phi_{np}(\vec{r})|V_{np}(\vec{r})|\phi_{np}(\vec{r})\rangle}, \quad (2)$$

where U_{nB} and U_{pB} are the neutron and proton optical model potentials on the target nucleus B evaluated at half the deuteron incident energies (the "$E_d/2$ rule"). Thus, nucleon OMPs for the p-A, p-B, and n-B systems are required in a $A(p,d)B$ reaction.

For most existing studies employing TBMRM, the zero-range (ZR) adiabatic potential was used in the ADWA calculations. In the zero-range version of the ADWA, the effective deuteron potential simply becomes

$$U_{dB}(R) = U_{nB}(R) + U_{pB}(R). \quad (3)$$

However, the systematic calculations performed by Nguyen *et al.* [20] show that finite-range effects may become more significant with increased beam energies. Therefore, the finite-range version of the adiabatic potential is applied in this study.

Table 1 shows the global systematics of all nucleon OMPs used in this study to analyze the transfer data. Microscopic OMPs of JLM [15] and CTOM [22] are employed for proton and neutron potentials with nucleon density distributions given by HF calculations. The real and imaginary parts of the JLM potentials are scaled with the conventional factors $\lambda_V = 1.0$ and $\lambda_W = 0.8$ [10, 33]. Notably, although the WLH potential should work for incident energies below 150 MeV, our previous study showed that it could reasonably reproduce the transfer data for higher energies at forward angles. Therefore, we choose the global phenomenological OMP KD02 [34].

The optical potential should be non-local to enable more realistic descriptions of the reaction mechanism. Non-locality corrections with a range parameter of 0.85 fm obtained by fitting the experimental data are included in the proton channel. The common deuteron potential non-locality correction parameter is not recommended in an adiabatic description of the deuteron channel, so this study does not consider the non-locality of the deuteron OMP.

The single particle wave functions are calculated using the separation energy prescription with the Woods-Saxon form of single particle potentials. The depths of these potentials are adjusted to reproduce the separation energies of the neutron in the ground states of the target nuclei. The radius and diffuseness parameters of these potentials, r_0 and a_0, are also important for nuclear transfer reactions. Their empirical values are $r_0 = 1.25$ fm and $a_0 = 0.65$ fm. However, these empirical values cannot be expected to represent the specific structure of any single specific nucleus. A better solution is to confine the r_0 and a_0 values with reliable nuclear structure theory. The TBMRM constrains the r_0 and a_0 values using modern Hartree-Fock (HF) calculations [13, 35–40], fixing the diffuseness parameter at $a_0 = 0.65$ fm. The radius parameter r_0 is determined by requiring that the root mean square (RMS) radius of the single neutron wave function, $\sqrt{\langle r^2\rangle}$, is related to the RMS radius of the corresponding single particle orbital from the HF calculations, $\sqrt{\langle r^2\rangle_{\rm HF}}$, by $\langle r^2\rangle = [A/(A-1)]\langle r^2\rangle_{\rm HF}$. The $[A/(A-1)]$ factor is used to correct the fixed potential center assumption used in the HF calculations, where A is the mass number of the composite nucleus. All HF calculations in this study are based on the SkX interaction [41]. After r_0 and a_0 are determined, the depths of the single particle potentials are determined using experimental separation energies $S_n^{\rm exp}$. All calculations make the local energy approximation (LEA) for finite range effects using the normalization strength ($D_0 = -125.2$ MeV·fm$^{3/2}$) and range r ($\beta = 0.7457$ fm) parameters of the Reid soft-core $^3S_1$-$^3D^1$ neutron-proton interaction. The computer code TWOFNR [42] is adopted to calculate the differential cross sections.

The theoretical calculations with different sets of optical parameters can reasonably reproduce the experimental data. By matching these theoretical differential cross sections to the former at the largest experimental cross sections, the experimental SFs, SF$^{\rm exp}$, of the neutrons in the ground states of the reaction residues are obtained. The experimental angular distributions at larger angles are generally more sensitive to the optical potential details, inelastic coupling effects, and other higher order effects not well reproduced by most reaction models. Furthermore, discrepancies between the shapes from calculations and experiments are much worse at the cross section minimum. Thus, the spectroscopic factor is generally extracted by fitting the reaction model predictions to the angular distribution data at the first peak, emphasiz-

Table 1. Global systematics of nucleon optical potentials.

Projectile	Systematics	Type	Mass range	Energy range
p,n	JLM	semi-microscopic	$12 \leqslant A \leqslant 208$	$E \leqslant 200$ MeV
p,n	CTOM	semi-microscopic	$12 \leqslant A \leqslant 208$	$E \leqslant 200$ MeV
p,n	WLH	microscopic	$12 \leqslant A \leqslant 242$	$E \leqslant 150$ MeV
p,n	KD02	phenomenological	$24 \leqslant A \leqslant 209$	$E \leqslant 200$ MeV

ing the maximum. However, the accuracy of absolute cross section measurements near the peak is crucial. We take the mean of as many points near the maximum as possible to extract the spectroscopic factors. As an example, we show the analysis of the ^{12}C$(p,d)^{11}$C reaction at an incident energy of 30.3 MeV in Fig. 1 to illustrate the procedure for extracting the spectroscopic factors. In Fig. 1, the first four data points with $\theta < 30°$ have been used to determine the ratios of the measured and calculated differential cross sections. The mean value of these four ratios is adopted as the experimental SF, and the results are listed in Table 2.

The theoretical SFs and corresponding interactions used in the calculations are listed in Table 3. In this study, the theoretical spectroscopic factors are expressed as $\mathrm{SF}^{\mathrm{th}} = [A/(A-1)]^N \times C^2S(J^\pi, nlj)$, where the shell model spectroscopic factors $C^2S(J^\pi, nlj)$ are obtained from shell model calculations using the code OXBASH [43]. J^π denotes the spin-parties of the core states, and nlj represents the quantum numbers of the single particle states of the transferred nucleon. The $[A/(A-1)]^N$ factor is for center-of-mass corrections to the shell model SFs [44], where $N = 2n + l$ is the number of the oscillator quanta associated with the major shell of the removed particle and A is the mass number of the composite nucleus.

III. RESULTS AND DISCUSSIONS

The SFs extracted from experimental data are known to be quenched considerably compared with the predictions of independent particle or shell models for nuclei. In transfer reactions, the reduction factors of single-nucleon strengths R_s are defined as the ratio between the experimental and theoretical SFs: $R_s = \mathrm{SF}^{\mathrm{exp}}/\mathrm{SF}^{\mathrm{th}}$. Such quenching of single particle strengths has been attributed to some profound questions in nuclear physics, such as short- and medium-range nucleon–nucleon correlations and long-range correlations from the single-particle motion coupling of the nucleons near the Fermi surface and the collective excitations. Additionally, the reduction factors obtained from the transfer [10, 13, 38, 39, 45–48], single-nucleon removal [35, 36, 40, 49–53], and quasi-free knockout [54–60] reactions show varied dependence

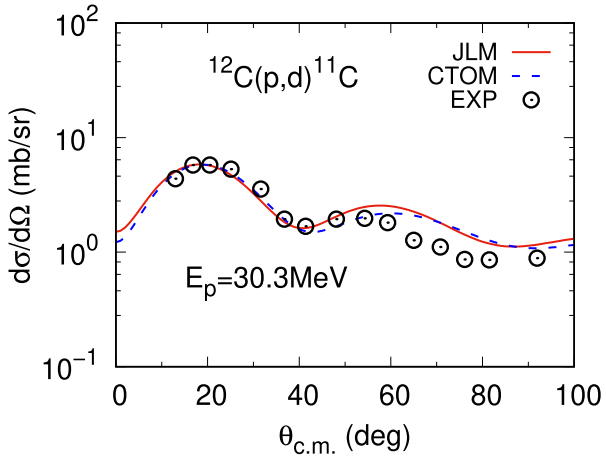

Fig. 1. (color online) Angular distributions of $^{12}C_{g.s.}(p, d)^{11}C_{g.s.}$ reaction at an incident proton energy of 30.3 MeV. The curved and dashed lines represent the theoretical results calculated by JLM and CTOM, multiplied by the corresponding spectroscopic factor separately.

Table 2. Experimental spectroscopic factors extracted from (p,d) reactions.

Target	E_p/MeV	$\mathrm{SF}^{\mathrm{exp}}$			
		JLM	CTOM	KD02	WLH
^{12}C	30.3	1.722	1.561	1.677	2.326
	51.93	2.163	1.528	2.326	2.751
	61	2.075	1.600	2.347	2.761
	65	2.170	1.598	2.339	2.651
	100	2.131	2.029	2.877	2.507
	122	1.335	1.437	2.498	1.529
	156	1.291	1.542	2.656	1.428
	185	0.753	1.030	1.784	0.871
^{16}O	20	1.324	0.869	1.380	1.234
	25.52	1.523	1.010	1.855	1.608
	30.3	1.161	0.903	1.232	1.364
	38.63	1.205	0.858	1.348	1.385
	45.34	1.279	0.977	1.441	1.495
	61	1.563	1.127	1.772	1.752
	65	1.447	1.054	1.640	1.605
	100	2.591	2.094	3.234	2.580
	155	2.203	2.498	3.947	2.058
	200	2.150	3.344	4.005	2.492
^{28}Si	33.6	2.816	2.139	3.883	3.820
	51.93	3.132	2.213	3.660	3.980
	65	2.412	1.592	2.320	3.119
	135	0.879	0.989	1.755	1.104
	185	0.869	1.158	1.923	1.014
^{40}Ca	27.5	2.829	2.031	2.854	2.974
	30.3	3.417	2.594	3.399	3.667
	33.6	4.299	3.238	4.498	4.691
	40	4.072	3.131	4.328	4.701
	51.93	3.749	2.796	3.928	4.343
	65	2.697	1.950	2.746	3.041
	156	3.199	3.678	4.656	2.926
	185	2.703	3.850	4.589	2.569
	200	2.091	2.225	3.986	2.100

Table 3. Shell model predicted spectroscopic factors, SF^{th}, and interactions used in shell model calculations.

Reaction	nlj	SF^{th}	Interaction
$^{12}C_{g.s.}(p,d)^{11}C_{g.s.}$	0p3/2	3.447	WBT
$^{16}O_{g.s.}(p,d)^{15}O_{g.s.}$	0p1/2	1.842	WBT
$^{28}Si_{g.s.}(p,d)^{27}Si_{g.s.}$	0d5/2	3.887	USD
$^{40}Ca_{g.s.}(p,d)^{39}Ca_{g.s.}$	0d3/2	3.885	SPDF-M

on proton-neutron asymmetry, which is still an open question [2].

Obviously, for transfer reactions, the R_s uncertainties result from the extraction of experimental spectroscopic factors. The quenching of single-nucleon SFs measured in $(e,e'p)$ reactions, which are free from the uncertainties of OMPs and are thus deemed to be more reliable, are known to range approximately between 0.4 and 0.7 [47, 61]. Therefore, SFs derived from a self-consistent analysis are expectedly quenched by a common factor of approximately 0.55 ± 0.10, independent of whether the reaction is nucleon adding or removing and whether a neutron or proton is transferred; in addition, the quenching is independent of the mass of the nucleus, reaction type, and angular momentum transfer [47, 61]. This study assesses the stability of SF^{exp} extracted from (p,d) reactions by comparing R_s with the systematics of the $(e,e'p)$ reactions. The R_s values are plotted as a function of the incident energy for different targets in Figs. 2−5. The open circles represent the results calculated using microscopic and phenomenological OMPs.

Overall, one observes that the R_s values under different OMPs show no significant incident energy dependence when $E < 70$ MeV, which is consistent with the results of Ref. [39]. However, there are only three points for ^{28}Si, and the $R_s$values of ^{40}Ca scatter considerably, although they are obtained using the same methodology wherein all reactions are analyzed with the same procedure without free parameters. However, new precision measurements will be helpful. Satisfactorily, the results with CTOM agree well with the systematics of $(e,e'p)$ reactions at low energies, which is also the energy range of most previous systematic analyses of (d,p) and (p,d) reactions [9, 11, 38, 39]. Therefore, reanalyzing previous studies by applying CTOM would be worthwhile. However, the situation becomes more complex with increased beam energy. To gain a clear understanding, the R_s/SF values are fitted by a linear function of the incident energies, and the results are listed in Table 4. Figure 6 shows the slope parameters from linear fits of spectroscopic factors obtained using different OMPs. The R_s/SF values obtained by phenomenological OMP KD02 and old microscopic OMP JLM exhibit clear decreases for ^{12}C, ^{28}Si, and ^{40}Ca and a clear increase for ^{16}O, with incident energy increase. This outcome is inconsistent with the

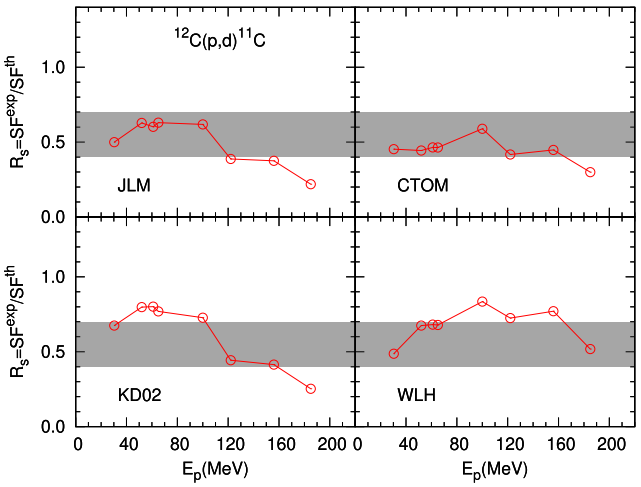

Fig. 2. (color online) Reduction factors of the single neutron spectroscopic factors for $^{12}C_{g.s.}(p,d)^{11}C_{g.s.}$, with different OMPs indicated in the figures. The grey area represents the totality of the bulk of R_s for the $(e,e'p)$ from Refs. [47, 61] to guide the eye.

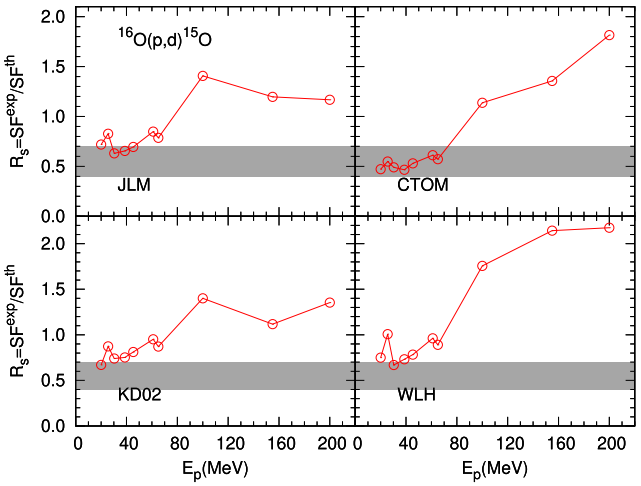

Fig. 3. (color online) Same as Fig. 2 but for $^{16}O_{g.s.}(p,d)^{15}O_{g.s.}$.

results in knockout reactions, where no strong incident energy dependence is observed in the R_s values within a wide energy range (43−2100 MeV/nucleon) [40]. This significant energy dependence reduces significantly when new microscopic OMPs are employed in the calculations, except for ^{16}O. Notably, noticeable discrepancies are observed in the experimental SF values calculated using new microscopic OMPs compared with those resulting from KD02 and JLM when $E \geq 100$ MeV/nucleon, especially for ^{16}O and ^{40}Ca.

As stated above, no significant difference in the extraction of SF values is observed between the semi-microscopic potential JLM and the phenomenological potential KD. This is not surprising since neutron capture rate calculations using the KD02 and JLM also give similar results [62]. Although JLM has showed good predict-

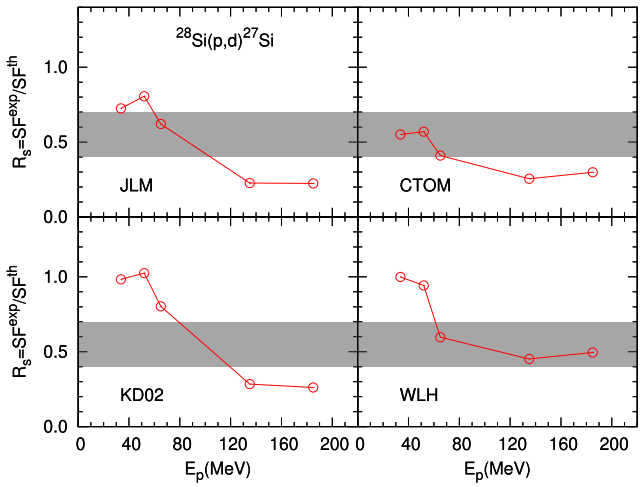

Fig. 4. (color online) Same as Fig. 2 but for $^{28}\mathrm{Si}_{\mathrm{g.s.}}(p,d)^{27}\mathrm{Si}_{\mathrm{g.s.}}$.

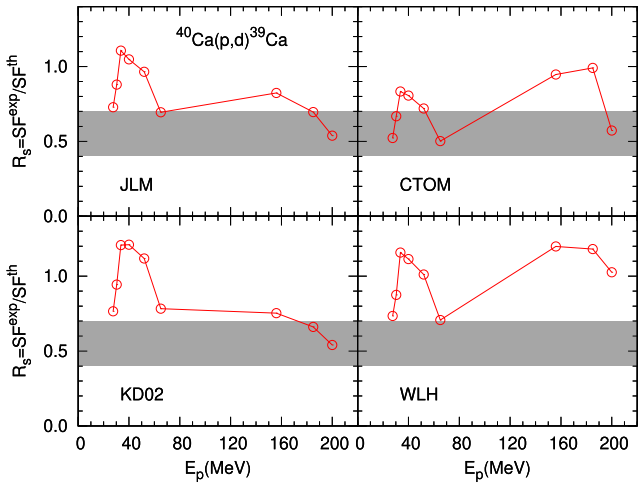

Fig. 5. (color online) Same as Fig. 2 but for $^{40}\mathrm{Ca}_{\mathrm{g.s.}}(p,d)^{39}\mathrm{Ca}_{\mathrm{g.s.}}$.

ive power for scattering and transfer reactions, its precision hardly improves beyond using better nuclear structure input, and it relies on simplified nuclear matter calculations with old-fashioned bare interactions, owing to its phenomenological aspect.

The new microscopic OMPs, CTOM, and WLH, constructed from modern nuclear matter calculations, may provide an anticipated prospect. CTOM potential parameters can provide credible SFs with a smaller energy dependence and better consistency with the results of $(e,e'p)$ reactions at low energy regions. Results calculated using WLH tend to be similar but generally larger than those using CTOM parameters. However, the nuclear matter approach omits surface effects, resonances, and spin–orbit interactions and tends to produce an overly absorptive imaginary term at high energies. These shortcomings may lead to reduced performance at higher energies. Another discrepancy of the SFs occurs on the double-magic nuclei. Ref. [63] shows that, for the double-magic nuclei, the important contributions to SF result

Table 4. Spectroscopic factor slope parameters for different optical model potentials.

Target	slope /MeV^{-1}			
	JLM	CTOM	WLH	KD02
^{12}C	−0.008	−0.002	0.001	−0.012
^{16}O	0.006	0.014	0.017	0.007
^{28}Si	−0.016	−0.008	−0.013	−0.022
^{40}Ca	−0.007	0.003	0.005	−0.010

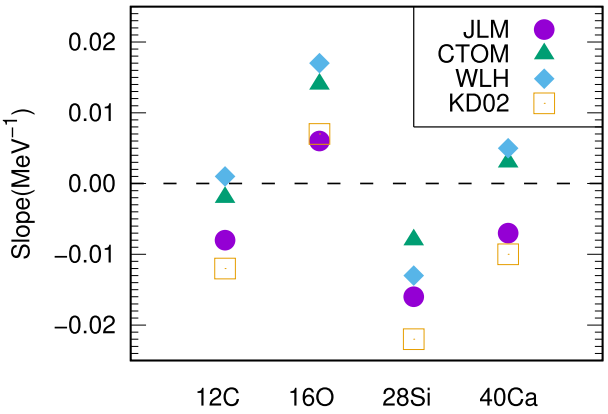

Fig. 6. (color online) Summary of spectroscopic factor slope parameters across different optical parameters.

mostly from the internal nuclear region. In contrast, the contribution resulting from the surface area should not be neglected for other nuclei. When a systematic potential is derived from large elastic scattering data extrapolated to other nuclei or other energy regions, it can usually reasonably reproduce these experimental data but cannot provide satisfactory results for double-magic nuclei, owing to their special properties. OMPs with double-magic nuclei are generally not known to follow the systematics of OMPs established for other nuclei owing to the relatively larger excitation energies of their first few excited states [64, 65]. Moreover, we note that the fitting of CTOM lacks the nucleon elastic scattering data for light nuclei at high energies; the CTOM predictions tend to underestimate the data for the differential cross section of ^{12}C-^{40}Ca above 120 MeV. However, these underestimations become more serious in ^{16}O and ^{40}Ca.

Notably, although ADWA is generally regarded as a reliable tool for describing transfer reactions in the non-relativistic energy region, previous applications have focused on the < 70 MeV/nucleon range. In Ref. [66], the discrepancy between the ADWA and Faddeev models was found to be much larger at 50 MeV/nucleon than at 28 MeV/nucleon in the $^{48}\mathrm{Ca}(d,p)^{49}\mathrm{Ca}$ case, resulting in larger SFs at higher energies, consistent with our present findings. A systematic analysis by solving the Faddeev-AGS equations would be interesting and may help to further understand the systematic discrepancy.

IV. SUMMARY

OMPs are important inputs in direct nuclear reaction calculations and have advanced significantly in recent years. This study conducted a systematic analysis fo 32 sets of angular distributions of (p,d) reactions on four even–even nuclei with energies ranging from 18 to 200 MeV/nucleon, within the ADWA framework. We investigate separately the effects of different OMPs on nuclear structure information derived from transfer reactions. Three microscopic OMPs and one phenomenological OMP are used in the analysis. Among them, JLM relies on simplified nuclear matter calculations with old-fashioned bare interactions, while CTOM and WLH have been recently proposed based on modern nuclear matter calculations. We find that spectroscopic values extracted from (p,d) reactions using JLM and phenomenological KD02 potential exhibit a strong energy dependence on beam energies. The incident energy dependence is suppressed when the new microscopic OMPs, CTOM, and WLH are employed, except for ^{16}O. Specifically, spectroscopic factors extracted using the systematic microscopic optical potential CTOM based on the Dirac-Brueckner-Hartree-Fock theory are consistent with results obtained from $(e,e'p)$ measurements, except for ^{16}O and ^{40}Ca at high energies ($\geq$ 100 MeV), necessitating an exact treatment of double-magic nuclei. The results obtained by using pure microscopic optical potential WLH based on EFT theory show the same trend but are generally higher than CTOM. Our results suggest the new microscopic optical potential based on modern nuclear matter approaches can effectively improve the extraction of the SFs and its reduction factors below 70 MeV/nucleon, compared with JLM folding potentials and phenomenological potentials KD02. Our study suggests that ongoing microscopic optical potentials based on more fundamental principles of nuclear interactions enable more reliable nuclear structure information than phenomenological OMPs and traditional semi-microscopic OMPS. Unfortunately, the CTOM and WLH potential parameters cannot give satisfactory results for double-magic nuclei or at high energies. The quality of the nuclei property description from optical potentials derived within the nuclear matter approach must be assessed using experimental data comparisons. Our work may also be valuable for such purposes.

This study leveraged the relatively simple ADWA model to compare the reduction factors. More rigorous theories, such as the continuum discretized coupled channels method (CDCC) and the Faddeev-AGS equations, may explain the systematic discrepancy at different energies. Additionally, the non-locality effects of the nucleon potentials and core excitations may not be neglected at higher energies. This study used HF calculations to constrain parameters that may not be optimal for some nuclei. Further studies on improved methodologies for the calculations will be interesting and are thus anticipated.

References

[1] N. K. Glendenning, *Direct Nuclear Reactions* (World Scientific, Singapore, 2004)
[2] T. Aumann, C. Barbieri, D. Bazin *et al*., Prog. Part. Nucl. Phys. **118**, 103847 (2021)
[3] H. C. Lee, *Survey of neutron spectroscopic factors and asymmetry dependence of neutron correlations in transfer reactions*, Ph.D. thesis, Michigan State University, USA, 2010
[4] F. M. Nunes, A. Deltuva, and J. Hong, Phys. Rev. C **83**, 034610 (2011)
[5] D. Y. Pang and A. M. Mukhamedzhanov, Phys. Rev. C **90**, 044611 (2014)
[6] A. E. Lovell, F. M. Nunes, J. Sarich *et al*., Phys. Rev. C **95**, 024611 (2017)
[7] G. B. King, A. E. Lovell, and F. M. Nunes, Phys. Rev. C **98**, 044623 (2018)
[8] N. Timofeyuk and R. Johnson, Prog. Part. and Nucl. Phys. **111**, 103738 (2020)
[9] X. D. Liu, M. A. Famiano, W. G. Lynch *et al*., Phys. Rev. C **69**, 064313 (2004)
[10] J. Lee, J. A. Tostevin, and B. A. Brown, Phys. Rev. C **73**, 044608 (2006)
[11] J. Lee, M. B. Tsang, and W. G. Lynch, Phys. Rev. C **75**, 064320 (2007)
[12] J. Lee, M. B. Tsang, W. G. Lynch *et al*., Phys. Rev. C **79**, 054611 (2009)
[13] J. Lee, M. B. Tsang, D. Bazin *et al*., Phys. Rev. Lett. **104**, 112701 (2010)
[14] R. C. Johnson and P.J. R. Soper, Phys. Rev. C **1**, 976 (1970)
[15] J.-P. Jeukenne, A. Lejeune, and C. Mahaux, Phys. Rev. C **16**, 80 (1977)
[16] E. Bauge, J. P. Delaroche, and M. Girod, Phys. Rev. C **63**, 024607 (2001)
[17] S. Dickey, J. Kraushaar, and M. Rumore, Nucl. Phys. A **391**, 413 (1982)
[18] S. Nakayama and Y. Watanabe, J. Nucl. Sci. Tech. **53**, 89 (2016)
[19] M. Yahiro, K. Ogata, T. Matsumoto *et al*., PTEP **126**, 167 (2011)
[20] N. B. Nguyen, F. M. Nunes, and R. C. Johnson, Phys. Rev. C **82**, 014611 (2010)
[21] X. Y. Yun, D. Y. Pang, Y. P. Xu *et al*., Sci. China Phys. Mech. Astron. **63**, 222011 (2020)
[22] R. R. Xu, Z. Y. Ma, Y. Zhang *et al*., Phys. Rev. C **94**, 034606 (2016)
[23] T. R. Whitehead, Y. Lim, and J. W. Holt, Phys. Rev. Lett. **127**, 182502 (2021)
[24] W. L. J. Lee and M. B. Tsang, arXiv: nucl-ex/0511024
[25] Experimental nuclear reaction data(exfor/csisrs), [DB(DB/OL)].
[26] J. Lee, S. Mark, P. Portner *et al*., Nucl. Phys. A **106**, 357 (1967)

[27] J. R. Comfort and B. C. Karp, Phys. Rev. C **21**, 2162 (1980), [Erratum: Phys. Rev. C 22, 1809 (1980)]
[28] D. A. du texte Bachelier, M. Bernas, I. Brissaud *et al.*, Nucl. Phys. **126**, 60 (1969)
[29] A. Ingemarsson and G. Tibell, Phys. Scripta **10**, 159 (1974)
[30] R. Abegg, D. A. Hutcheon, C. A. Miller *et al.*, Phys. Rev. C **39**, 65 (1989)
[31] J. Källne and B. Fagerström, Phys. Scripta **11**, 79 (1975)
[32] R. Johnson and P. Tandy, Nucl. Phys. A **235**, 56 (1974)
[33] J. S. Petler, M. S. Islam, R. W. Finlay *et al.*, Phys. Rev. C **32**, 673 (1985)
[34] A. Koning and J. Delaroche, Nuclear Physics A **713**, 231 (2003)
[35] J. A. Tostevin and A. Gade, Phys. Rev. C **103**, 054610 (2021)
[36] Y. Z. Sun, S. T. Wang, Z. Y. Sun *et al.*, Phys. Rev. C **104**, 014310 (2021)
[37] Y. Z. Sun, S. T. Wang, Y. P. Xu *et al.*, Phys. Rev. C **106**, 034614 (2022)
[38] Y. P. Xu, D. Y. Pang, X. Y. Yun *et al.*, Phys. Lett. B **790**, 308 (2019)
[39] J. Manfredi, J. Lee, A. M. Rogers *et al.*, Phys. Rev. C **104**, 024608 (2021)
[40] Y.-P. Xu, D.-Y. Pang, C.-X. Yuan *et al.*, Chin. Phys. C **46**, 064102 (2022)
[41] B. A. Brown, Phys. Rev. C **58**, 220 (1998)
[42] J. Tostevin, *Computer code TWOFNR* (University of Surrey version, 1977) https://people.nscl.msu.edu/~brown/reaction-codes/twofnr/twofnr.pdf
[43] B. A. Brown, A. Etchegoyen, and W. D. M. Rae, *Computer code OXBASH* (the Oxford University- Buenos Aires-MSU shell model code, 1985) https://people.nscl.msu.edu/~brown/resources/MSU-NSCL-Report-No-1289-2004.pdf
[44] A. E. L. Dieperink and T. d. Forest, Phys. Rev. C **10**, 543 (1974)
[45] M. B. Tsang, J. Lee, S. C. Su *et al.*, Phys. Rev. Lett. **102**, 062501 (2009)
[46] F. Flavigny, A. Gillibert, L. Nalpas *et al.*, Phys. Rev. Lett. **110**, 122503 (2013)
[47] B. P. Kay, J. P. Schiffer, and S. J. Freeman, Phys. Rev. Lett. **111**, 042502 (2013)
[48] F. Flavigny, N. Keeley, A. Gillibert *et al.*, Phys. Rev. C **97**, 034601 (2018)
[49] A. Gade, P. Adrich, D. Bazin *et al.*, Phys. Rev. C **77**, 044306 (2008)
[50] E. C. Simpson and J. A. Tostevin, Phys. Rev. C **79**, 024616 (2009)
[51] J. A. Tostevin and A. Gade, Phys. Rev. C **90**, 057602 (2014)
[52] R. J. Charity, L. G. Sobotka, and J. A. Tostevin, Phys. Rev. C **102**, 044614 (2020)
[53] J. Díaz-Cortés, J. Benlliure, J. L. Rodríguez-Sánchez *et al.*, Phys. Lett. B **811**, 135962 (2020)
[54] L. Atar, S. Paschalis, C. Barbieri *et al.*, Phys. Rev. Lett. **120**, 052501 (2018)
[55] M. Gómez-Ramos and A. Moro, Physics Letters B **785**, 511 (2018)
[56] S. Kawase, T. Uesaka, T. L. Tang *et al.*, PTEP **2018**, (2018)
[57] N. T. T. Phuc, K. Yoshida, and K. Ogata, Phys. Rev. C **100**, 064604 (2019)
[58] M. Holl, V. Panin, H. Alvarez-Pol *et al.*, Phys. Lett. B **795**, 682 (2019)
[59] C. A. Bertulani, A. Idini, and C. Barbieri, Phys. Rev. C **104**, L061602 (2021)
[60] J. Li, C. A. Bertulani, and F. Xu, Phys. Rev. C **105**, 024613 (2022)
[61] G. Kramer, H. Blok, and L. Lapikas, Nucl. Phys. A **679**, 267 (2001)
[62] C. Hebborn, F. M. Nunes, G. Potel *et al.*, J. Phys. G: Nucl. Part. Phys. **50**, 060501 (2023)
[63] N. K. Timofeyuk, J. Phys. G: Nucl. Part. Phys. **41**, 094008 (2014)
[64] R. Varner, W. Thompson, T. McAbee *et al.*, Phys. Rep. **201**, 57 (1991)
[65] D. Y. Pang, P. Roussel-Chomaz, H. Savajols *et al.*, Phys. Rev. C **79**, 024615 (2009)
[66] F. M. Nunes and A. Deltuva, Phys. Rev. C **84**, 034607 (2011)